Biochemical and Biophysical Research Communications 451 (2014) 152–157

Contents lists available at ScienceDirect

Biochemical and Biophysical Research Communications

journal homepage: www.elsevier.com/locate/ybbrc

Structural and functional characterization of *Streptococcus pyogenes* Cas2 protein under different pH conditions

Donghyun Ka [a], Dayoun Kim [b], Gyeongyun Baek [b], Euiyoung Bae [a,c,d,*]

[a] Department of Agricultural Biotechnology, Seoul National University, Seoul 151-921, Republic of Korea
[b] Department of Applied Biology and Chemistry, Seoul National University, Seoul 151-921, Republic of Korea
[c] Center for Food and Bioconvergence, Seoul National University, Seoul 151-921, Republic of Korea
[d] Research Institute of Agriculture and Life Sciences, Seoul National University, Seoul 151-921, Republic of Korea

ARTICLE INFO

Article history:
Received 8 July 2014
Available online 29 July 2014

Keywords:
CRISPR
Cas
Streptococcus pyogenes
Deoxyribonuclease
Structural biology

ABSTRACT

Clustered regularly interspaced short palindromic repeats (CRISPRs) and CRISPR-associated (Cas) proteins constitute an RNA-guided microbial defense system against invading foreign genetic materials. Cas2 is one of the core Cas proteins found universally in all the subtypes of CRISPR-Cas systems and is required for incorporating new spacers into CRISPR loci. Cas2 homologues from different CRISPR-Cas subtypes were characterized previously as metal-dependent nucleases with different substrate preferences, and it was proposed that a pH-dependent conformational change mediates metal binding and catalysis. Here, we report the crystal structures of *Streptococcus pyogenes* Cas2 at three different pHs (5.6, 6.5, and 7.5), as well as the results of its nuclease activity assay against double-stranded DNAs at varying pHs (6.0–9.0). Although *S. pyogenes* Cas2 exhibited strongly pH-dependent catalytic activity, there was no significant conformational difference among the three crystal structures. However, structural comparisons with other Cas2 homologues revealed structural variability and the flexible nature of its putative hinge regions, supporting the hypothesis that conformational switching is important for catalysis. Taken together, our results confirm that Cas2 proteins have pH-dependent nuclease activity against double-stranded DNAs, and provide indirect structural evidence for their conformational changes.

1. Introduction

Clustered regularly interspaced short palindromic repeats (CRISPRs) form an RNA-guided microbial defense system against invading foreign genetic materials [1,2]. CRISPRs are a class of repetitive elements found within many archaeal and bacterial genomes. They consist of a few to hundreds of invariable 'repeat' sequences interspaced with variable 'spacer' sequences, some of which match sequences within foreign nucleic acids. CRISPR-associated (*cas*) genes are located adjacent to CRISPR loci and encode Cas proteins with various nucleic acid-related functions.

CRISPRs and Cas proteins provide adaptive immunity against invading foreign genetic elements, such as phages and plasmids, via a three-stage mechanism [1–3]. In the adaptation stage, foreign nucleic acid fragments are integrated into the host genome as spacers within the CRISPR loci, which are then transcribed and processed to generate small CRISPR RNAs during the expression stage. In the interference stage, these CRISPR RNAs are used as guides for recognizing and degrading the foreign nucleic acids. The roles of Cas proteins in the adaptation stage are relatively poorly understood while their mechanisms and functions in the expression and interference stages have been elucidated in greater detail [3,4].

Cas2 is one of the two core Cas proteins found universally in all CRISPR-Cas subtypes [5]. Cas1, the other universal Cas protein, and Cas2 are required for incorporating new spacers into CRISPR loci [6–8], suggesting that they have critical and conserved role(s) during the adaptation stage. The structural and functional characterization of Cas2 has been performed for several homologues, including those from *Sulfolobus solfataricus*, *Desulfovibrio vulgaris*, and *Bacillus halodurans* (SsCas2, DvCas2, and BhCas2, respectively) [9–11]. The Cas2 homologues share common structural features such as homodimeric assembly, an N-terminal ferredoxin fold, the swapping of C-terminal segments for dimerization, and a pair

Abbreviations: CRISPR, clustered regularly interspaced short palindromic repeats; Cas, CRISPR-associated; SsCas2, *Sulfolobus solfataricus* Cas2; DvCas2, *Desulfovibrio vulgaris* Cas2; BhCas2, *Bacillus halodurans* Cas2; SpCas2, *Streptococcus pyogenes* Cas2; ss, single-stranded; ds, double-stranded; DNase, deoxyribonuclease.

* Corresponding author at: Department of Agricultural Biotechnology, Seoul National University, Seoul 151-921, Republic of Korea. Fax: +82 2 873 3112.
E-mail address: bae@snu.ac.kr (E. Bae).

http://dx.doi.org/10.1016/j.bbrc.2014.07.087
0006-291X/

of conserved catalytic Asp residues. Several Cas2 proteins exhibited metal-dependent nuclease activities, but their substrate preferences differed markedly. SsCas2 cleaved single-stranded RNAs (ssRNAs) with a preference for U-rich sequences [9], but no such activity was observed with DvCas2 or BhCas2 [10,11]. In contrast, BhCas2 possesses non-specific nuclease activity toward double-stranded DNAs (dsDNAs) [11].

Conformational differences have also been recognized among Cas2 homologues, including the relative orientation of the protomers at the dimer interface. In the crystal structure of SsCas2, the side chains of the catalytic Asp10 residues from each protomer are located relatively adjacent to each other (6.5 Å), supporting the hypothesis that these two symmetric Asp residues coordinate a single divalent metal ion for catalysis [9]. However, in DvCas2 and BhCas2, rigid-body rotations were detected between two protomers, resulting in greater separations (15.4 and 10.6 Å, respectively) between the equivalent Asp residues [10,11]. In a previous study of BhCas2, Nam et al. performed a series of biochemical and biophysical experiments and proposed that a pH-dependent conformational change leads to association between the two Asp residues for metal binding and catalysis [11].

Here, we report the structural and functional characterization of *Streptococcus pyogenes* Cas2 (SpCas2) at varying pHs. We performed nuclease activity assays against dsDNAs at pH 6.0–9.0 and determined the crystal structures at three different pHs (5.6, 6.5, and 7.5). Although SpCas2 exhibited strongly pH-dependent catalytic activity, no significant conformational changes were observed among the three SpCas2 crystal structures. However, a structural comparison between SpCas2 and other homologues revealed structural variability and flexibility of its putative hinge regions, suggesting that conformational switching might occur. Taken together, our results confirm that SpCas2 exhibits pH-dependent nuclease activity against dsDNAs and provide indirect evidence for conformational changes.

2. Materials and methods

2.1. Cloning, expression and purification

The *S. pyogenes cas2* gene was amplified from *S. pyogenes* SF370 genomic DNA using polymerase chain reaction and was cloned into a pET21a vector with a C-terminal $(His)_6$ tag. *Escherichia coli* BL21 (DE3) cells harboring this construct were cultured in LB medium at 37 °C until the optical density at 600 nm reached 0.7. Protein expression was then induced by the addition of 0.3 mM isopropyl-β-D-thiogalactopyranoside, followed by incubation at 17 °C for 16 h. The cells were harvested by centrifugation and resuspended in lysis buffer (200 mM NaCl, 5 mM β-mercaptoethanol (BME), 20 mM MES pH 6.0).

After sonication and centrifugation, the supernatant was loaded onto a 5 mL HisTrap HP column (GE Healthcare) pre-equilibrated with elution buffer (200 mM NaCl, 5 mM BME, 30 mM imidazole, 20 mM MES pH 6.0). After washing the column with the elution buffer, the bound protein was eluted by applying a linear gradient of imidazole (up to 500 mM). The Cas2 protein was further purified using a HiLoad 16/60 Superdex75 column (GE Healthcare) equilibrated with size exclusion chromatography buffer (200 mM NaCl, 2 mM DTT, 20 mM MES pH 6.0).

2.2. DNA cleavage assays

Linearized pUC19 plasmids (100 ng) were incubated with SpCas2 proteins in reaction buffer (100 mM KCl, 2.5 mM $MgCl_2$, 20 mM Tris–HCl pH 8.0) at 37 °C for 1 h. For the assays at different pHs, MES (pH 6.0), HEPES (pH 7.0) and CHES (pH 9.0) buffers were used instead of Tris–HCl. After phenol–chloroform extraction, the reaction products were analyzed on 1% (w/v) agarose gels and visualized using ethidium bromide staining.

2.3. Crystallization, data collection, and structure determination

SpCas2 crystals were grown at 20 °C using the sitting-drop method from 9 mg/mL protein solution in buffer (200 mM KCl, 2 mM DTT, 20 mM MES pH 6.0) mixed with an equal volume of one of three reservoir solutions containing different pH buffers (5.6, 6.5, and 7.5). The pH 5.6 crystallization condition contained 30% (w/v) PEG 4000, 200 mM ammonium acetate, and 100 mM tri-sodium citrate pH 5.6. The pH 6.5 solution consisted of 30% (w/v) PEG 8000, 200 mM sodium acetate, and 100 mM sodium cacodylate pH 6.5. The pH 7.5 reservoir solution included 25% (w/v) PEG 3350, 200 mM $MgCl_2$, and 100 mM HEPES pH 7.5. The crystals were flash-frozen in liquid nitrogen without additional cryoprotecting reagents.

Diffraction data were collected at the beamline 7A of the Pohang Accelerator Laboratory at 100 K. The diffraction images were processed with HKL2000 [12]. The *B. halodurans* Cas2 structure (PDB code 4ES2) was used as a starting model for molecular replacement phasing in PHASER [13]. The final structures were completed using alternate cycles of manual fitting in COOT [14] and refinement in REFMAC5 [15]. The stereochemical quality of the final models was assessed using MolProbity [16].

2.4. Accession numbers

The atomic coordinates and structure factors of SpCas2 at pH 5.6, 6.5 and 7.5 were deposited in the Protein Data Bank [17] with the accession codes 4QR0, 4QR1, and 4QR2, respectively.

3. Results

3.1. Nuclease activity assays of SpCas2 against dsDNAs

We used linearized pUC19 plasmids as the substrates to examine the nuclease activity of SpCas2 against dsDNAs. In this assay, SpCas2 exhibited double-stranded deoxyribonuclease (dsDNase) activity (Fig. 1). DNA cleavage was enhanced with increasing concentrations of SpCas2 (Fig. 1A). The addition of EDTA prevented cleavage (Fig. 1B), suggesting that the DNase activity of SpCas2 is metal dependent. These observations were consistent with the previous study of BhCas2 [11]. It is noteworthy that both SpCas2 and BhCas2 belong to the subtype I-C CRISPR-Cas systems [5], suggesting that the choice of substrate might be subtype specific. Consistent with this, *Xanthomonas oryzae* Cas2, another homologue belonging to the subtype I-C CRISPR-Cas system [5], also exhibited dsDNase activity (Fig. S1).

Next, cleavage assays against dsDNAs were performed at different pHs (6.0–9.0) to determine whether the dsDNase activity of SpCas2 was pH-dependent, as was shown previously for BhCas2 [11]. The experiment revealed that the dsDNase activity of SpCas2 varied with pH (Fig. 1C). Activity was not, or only slightly, detectable at pHs 6.0 and 7.0, whereas cleavage increased dramatically at higher pHs, and was maximal at pH 8.0. Taken together, these results suggest that SpCas2 is a metal- and pH-dependent dsDNase that shares common functional features with the closely related Cas2 homologue, BhCas2.

3.2. Crystal structures of SpCas2 at different pHs

To assess the structural basis of the pH-dependent dsDNase activity in SpCas2, we determined its crystal structure using three

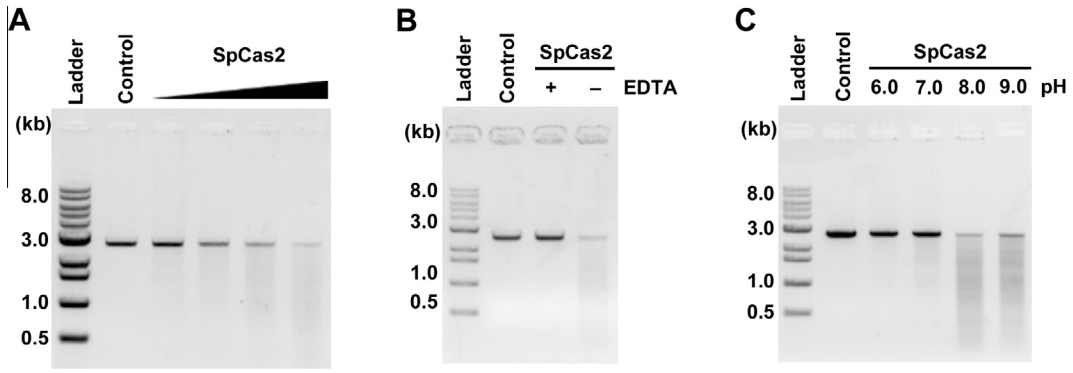

Fig. 1. Nuclease activity of SpCas2 against dsDNAs. (A) Cleavage of dsDNAs by SpCas2. Linearized pUC19 plasmids (100 ng) were incubated with increasing amounts (8, 16, 32, and 64 μM) of SpCas2. (B) Metal dependence of SpCas2 nuclease activity against dsDNAs. Linearized pUC19 plasmids (100 ng) were incubated with SpCas2 (64 μM) in the presence or absence of EDTA. (C) pH dependence of SpCas2 nuclease activity against dsDNAs. Linearized pUC19 plasmids (100 ng) were incubated with SpCas2 (64 μM) at different pHs.

crystallization conditions containing different pH buffers (5.6, 6.5, and 7.5). Data collection and refinement statistics are summarized in Table 1. All the three crystal structures belong to the $P4_12_12$ space group and contain two SpCas2 protomers forming a single dimer with a non-crystallographic twofold symmetry in their asymmetric units. The dimeric state of SpCas2 was also supported by the result from the size-exclusion chromatographic data (Fig. S2). Several C-terminal residues (residues 84–97 in protomer A and residues 83–97 in protomer B) and $(His)_6$ tags were not modeled in the final structures due to insufficient electron density.

Despite the differences in their crystallization conditions, the three SpCas2 dimers display essentially identical structural features, including topology and protomer fold, dimerization interface, and conformational state (Fig. S3). The SpCas2 protomers possess an N-terminal ferredoxin fold consisting of a four-stranded antiparallel β-sheet (β1–4) and two α-helices (α1, α2), followed by a C-terminal segment containing a 3_{10}-helix (η1) and a β-strand (β5) (Fig. 2A). The root mean square deviation (RMSD) values of Cα atomic positions between the SpCas2 protomers range from 0.1 to 0.3 Å. The C-terminal β5 strand in one protomer interacts with the β4 strand of the four-stranded β-sheet of the other protomer, forming two five-stranded antiparallel β-sheets in a single SpCas2 dimer (Fig. 2B). The interactions at the dimer interface are mostly between residues in the two β–sheets and are very similar in the three SpCas2 structures. The dimerization buries 2793–2856 $Å^2$ of the total surface area and forms 29–32 hydrogen bonds between the two protomers.

The conformational states of the three SpCas2 structures are also nearly identical (Fig. S3). The RMSD values among the three dimers ranges from 0.3 to 0.4 Å, even though they were crystallized at different pHs at which the catalytic activity varied significantly. This was somewhat surprising, because the previous study of BhCas2 strongly supported the hypothesis that a pH-dependent conformational change was required for the association of two symmetric Asp residues in order to coordinate a single divalent cation for catalysis [11]. The distances between the side chains of the equivalent Asp8 residues are 11.3, 11.8, and 11.4 Å in the SpCas2 dimers crystallized at pH 5.6, 6.5, and 7.5, respectively (Fig. 2B). Therefore, all of the three SpCas2 structures seem to exhibit catalytically inactive conformational states.

Table 1
Data collection and refinement statistics.[a]

	pH 5.6	pH 6.5	pH 7.5
Space group	$P4_12_12$	$P4_12_12$	$P4_12_12$
Unit cell parameters (Å)	$a = b = 54.8$ $c = 124.0$	$a = b = 55.1$, $c = 117.2$	$a = b = 55.3$, $c = 117.8$
Wavelength (Å)	0.9793	0.9793	0.9793
Data collection statistics			
Resolution range (Å)	50.00–2.40 (2.49–2.40)	50.00–2.20 (2.28–2.20)	50.03–1.80 (1.86–1.80)
Number of reflections (measured/unique)	106548/7806	121800/9551	242885/17673
Completeness (%)	98.1 (97.8)	96.8 (100.0)	99.8 (100.0)
R_{merge}[b]	0.098 (0.624)	0.118 (0.538)	0.072 (0.621)
Redundancy	13.6 (14.3)	12.8 (13.6)	13.7 (14.0)
Mean I/σ	20.50 (4.43)	15.55 (6.58)	35.2 (4.6)
Refinement statistics			
Resolution range (Å)	50.13–2.40	49.83–2.19	50.03–1.80
R_{cryst}[c]/R_{free}[d] (%)	19.6/24.6	20.7/26.7	18.3/23.4
RMSD bonds (Å)	0.014	0.015	0.020
RMSD angles (deg)	1.637	1.677	1.878
Average B factor ($Å^2$)	42.48	40.46	27.10
Number of water molecules	30	49	148
Ramachandran favored (%)	100.0	100.0	100.0
Ramachandran allowed (%)	0.0	0.0	0.0

[a] Values in parentheses are for the highest-resolution shell.
[b] $R_{merge} = \Sigma_h\Sigma|I_i(h) - \langle I(h)\rangle|/\Sigma_h\Sigma_i I_i(h)$, where $I_i(h)$ is the intensity of an individual measurement of the reflection and $\langle I(h)\rangle$ is the mean intensity of the reflection.
[c] $R_{cryst} = \Sigma_h||F_{obs}|-|F_{calc}||/\Sigma_h|F_{obs}|$, where F_{obs} and F_{calc} are the observed and calculated structure factor amplitudes, respectively.
[d] R_{free} was calculated as R_{cryst} using 5% of the randomly selected unique reflections that were omitted from structure refinement.

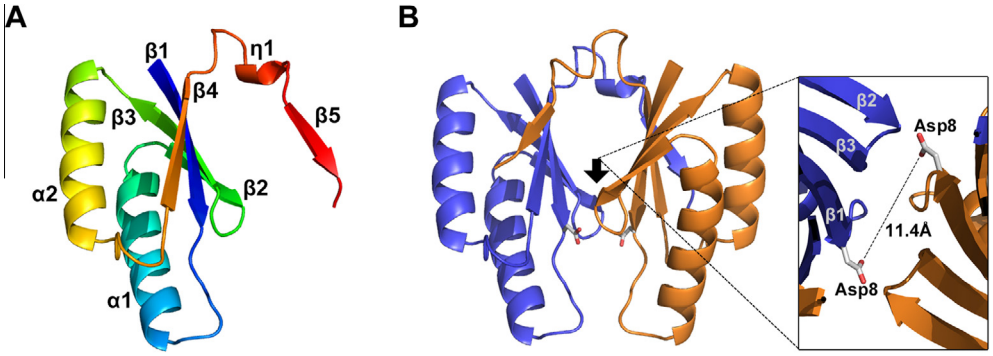

Fig. 2. Crystal structure of SpCas2. Structures of (A) SpCas2 protomer and (B) dimer. The structure crystallized at pH 7.5 is shown with the distance between the two Asp8 residues.

3.3. Structural comparison of SpCas2 with other Cas2 homologues

To further investigate the possibility that SpCas2 has multiple conformational states, we compared its structure with those of two highly homologous proteins, DvCas2 and BhCas2. Multiple structures obtained from different crystallization conditions were available for BhCas2 [11] as well as our SpCas2 structures. Therefore, we used those determined at the highest resolution (1.1 and 1.8 Å for BhCas2 and SpCas2, respectively) for the comparison.

Although the source organisms of the three Cas2 homologues are not closely related, all three Cas2 proteins belong to subtype I-C CRISPR-Cas systems [5], and SpCas2 shares ~50% sequence identity with DvCas2 and BhCas2 (Fig. 3A). The structural alignment of the three Cas2 homologues revealed that their overall structures are similar (Fig. 3B). The RMSD values of the Cα atoms between the SpCas2 structure and those of the DvCas2 and BhCas2 structures are 2.7 and 1.3 Å, respectively. All three proteins appear to be in catalytically inactive conformational states, as indicated by the large separations (>10 Å) between the two Asp residues critical for metal binding and catalysis.

Several structural deviations were also identified among the Cas2 homologues. The most notable differences were observed in the regions connecting the β4 and β5 strands (Fig. 3C). A structural comparison of the SpCas2 and DvCas2 protomers revealed a significant deviation in the positioning of the β5 strands, suggesting that the β5 strand can rotate, using its N-terminus as a fixed point. In

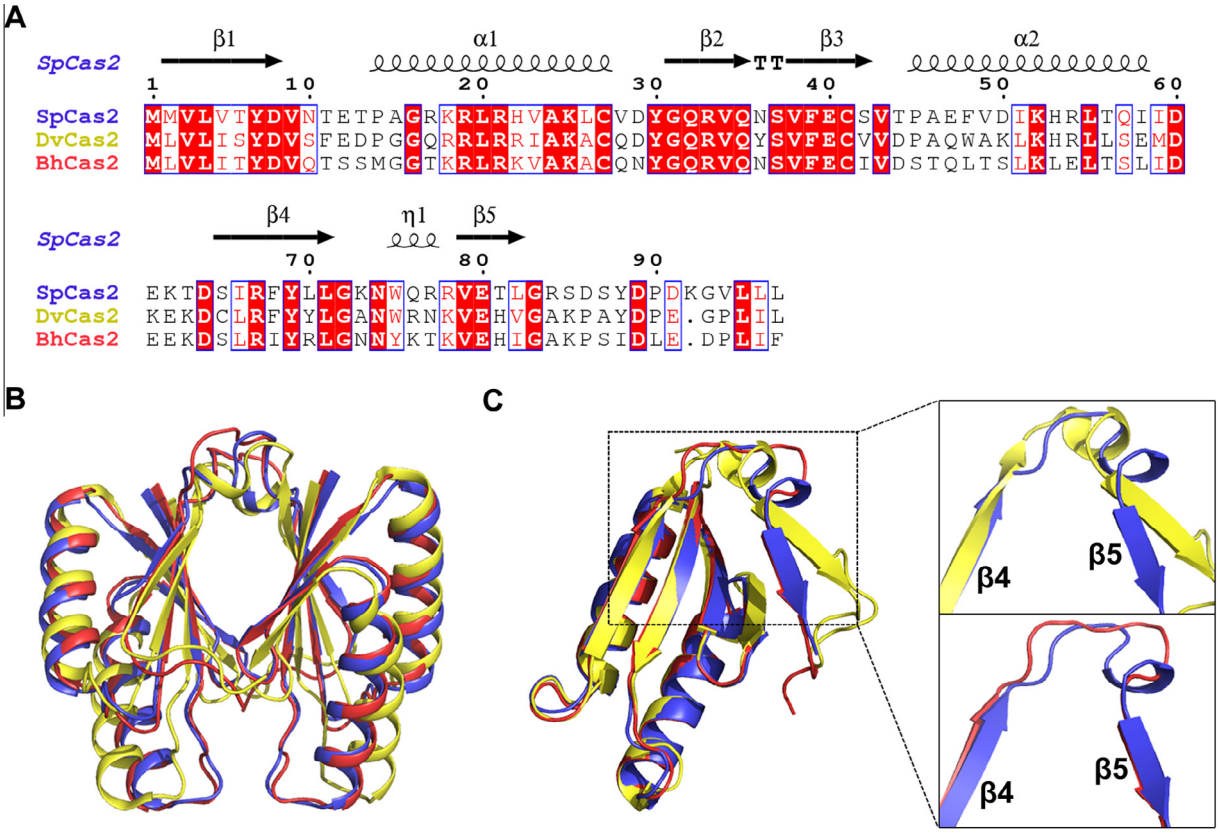

Fig. 3. Sequence alignment and structural comparison of Cas2 homologues. (A) Sequence alignment of SpCas2, DvCas2 and BhCas2 proteins. Secondary structures are indicated based on the SpCas2 structure. (B) Superposition of SpCas2 (blue), DvCas2 (yellow), and BhCas2 (red) dimers. (C) Structural variability of the putative hinge region in SpCas2 (blue), DvCas2 (yellow) and BhCas2 (red) protomers. (For interpretation of the references to colour in this figure legend, the reader is referred to the web version of this article.)

the dimeric structures, this hinge-bending motion causes the rotation of the other protomer, in which the deviation is maximized at the β1-α1 and α2-β4 loop regions. When the SpCas2 and DvCas2 dimers were aligned structurally based on only one of their two protomers, the distance between the two α1 N-termini is 10.6 Å, and the RMSD value between the equivalent Cα atoms in the other protomer is 5.9 Å. This conformational difference causes a more significant separation of the two catalytically crucial Asp residues in DvCas2 than in SpCas2. Specifically, the distances between the Asp residues are 15.4 and 11.4 Å in DvCas2 and SpCas2, respectively.

No significant conformational differences were observed between the structures of SpCas2 and BhCas2 (Fig. 3B). When the structures were aligned based on one of the two protomers in their dimeric structures, the RMSD value of Cα positions in the other protomer was only 2.2 Å, suggesting that the structure of BhCas2 is in a very similar conformational state to that of SpCas2. The distances between the two critical Asp residues are also similar in BhCas2 (10.6 Å) and SpCas2 (11.4 Å). However, we were able to detect localized but possibly important structural variability in the residues connecting the β4 and β5 strands (Fig. 3C). SpCas2 contains a short 3_{10} helix, whereas no secondary structural element was found in BhCas2, suggesting that this putative hinge region is flexible. In the two lower-resolution (1.3 and 1.7 Å) structures of BhCas2, several residues of the corresponding regions were not modeled due to insufficient electron density [11], supporting the hypothesis that this region exhibits localized flexibility. Taken together, the structural comparisons of the three Cas2 homologues revealed both conserved and variable structural features, and provided indirect evidence for conformational switching within Cas2 proteins.

4. Discussion

Previous studies have revealed that Cas2 proteins possess nuclease activity but reported contradictory results for the presence of dsDNase function [9,11]. Beloglazova et al. characterized six Cas2 homologues, including SsCas2, but detected no nuclease activity against DNA substrates [9]. However, Nam et al. identified robust dsDNase activity in BhCas2 [11]. In the present study, we demonstrated that SpCas2 could cleave dsDNAs, which is consistent with the results from the BhCas2 study. The dsDNase activities of both BhCas2 and SpCas2 were dependent on the presence of a metal ion as well as the pH condition of the reaction [11]. These observations further strengthen that there is similarity between the two Cas2 homologues, which belong to subtype I-C CRISPR-Cas systems [5]. SsCas2 is a member of a subtype I-A CRISPR-Cas system [5]. Taken together, these data suggest that the substrate preference of Cas2 proteins might be subtype specific, and that Cas2 proteins likely function as nucleases capable of cleaving dsDNAs in subtype I-C CRISPR-Cas systems. This is supported by the identification of dsDNase activity in another subtype I-C homologue, Cas2 from *X. oryzae* (Fig. S1).

The dsDNase activity of SpCas2 seems to conform well to its essential role in the adaptation stage of CRISPR-mediated immunity, during which spacer acquisition occurs. The DNase activity might be needed for the fragmentation and/or processing of foreign invading DNAs into spacer precursors, whereas the ribonuclease activity found in SsCas2 would require an additional reverse transcription step for the acquisition of new spacers. The dsDNase activity might also be necessary for the cleavage of the CRISPR loci for the insertion of new spacers. However, it is also possible that the enzymatic activity of Cas2 is not required for the adaptation stage. The other universal Cas protein, Cas1, was also characterized as a metal-dependent DNase [18,19], and it might be responsible for cleaving dsDNA substrates, at least in some CRISPR-Cas systems. A recent study of an *E. coli* CRISPR-Cas system demonstrated that the Cas1 and Cas2 proteins form a stable complex, and that the enzymatic activity of Cas2 was not required for spacer acquisition [20].

In the present study, it was unexpected to discover the identical conformational states of SpCas2 at different pHs. The previous study of BhCas2 suggested that a pH-dependent conformational change converts Cas2 into a metal-bound catalytically active state [11]. Although SpCas2 displayed pH-dependent nuclease activity against dsDNAs (Fig. 1C), the three SpCas2 crystal structures were in the same conformational state, in which the separation between the two critical Asp residues was too large (>11 Å) to coordinate a single metal ion for catalysis. Therefore, it is unlikely that SpCas2 could perform its catalytic function in this conformational state, because metal binding involving two Asp residues seems to be crucial for the dsDNase activity. No metal ion was observed near either of the two separated Asp residues in any of the SpCas2 structures, and the addition of EDTA eliminated the dsDNase activity of SpCas2 in the activity assay (Fig. 1B).

All three SpCas2 structures in the current study were crystallized in the same conformational state, despite the differences in the crystallization conditions including buffer pHs. It is possible that both the catalytically active and inactive conformational states can exist simultaneously, interchangeably, and in different ratios regardless of pH. It is also possible that one of the two states could be more suitable for packing in the crystal lattice. In addition, the catalytically active conformation could be transient or energetically unfavorable in the absence of its dsDNA substrate. Interestingly, all of the available Cas2 structures belonging to subtype I-C CRISPR-Cas systems were crystallized in their catalytically inactive conformational states. The three BhCas2 crystal structures obtained using different crystallization conditions and the single DvCas2 crystal structure appear to be in the inactive conformational state as the SpCas2 structures, as indicated by the long distances (>10 Å) between the two critical Asp residues. To examine this further, the crystal structure of Cas2 at a more basic pH and/or with its dsDNA substrate should be determined.

Acknowledgments

We thank the staff of the beamline 7A of the Pohang Accelerator Laboratory for their support with data collection and Yoon Koo for help in cloning *cas2* genes. This work was supported by the Basic Science Research Program through the National Research Foundation of Korea (NRF) funded by the Ministry of Education, Science and Technology (2013R1A1A2010018) and the Cooperative Research Program for Agricultural Science & Technology Development funded by Rural Development Administration (PJ009781).

Appendix A. Supplementary data

Supplementary data associated with this article can be found, in the online version, at http://dx.doi.org/10.1016/j.bbrc.2014.07.087.

References

[1] R. Sorek, C.M. Lawrence, B. Wiedenheft, CRISPR-mediated adaptive immune systems in bacteria and archaea, Annu. Rev. Biochem. 82 (2013) 237–266.
[2] B. Wiedenheft, S.H. Sternberg, J.A. Doudna, RNA-guided genetic silencing systems in bacteria and archaea, Nature 482 (2012) 331–338.
[3] J. van der Oost, E.R. Westra, R.N. Jackson, B. Wiedenheft, Unravelling the structural and mechanistic basis of CRISPR-Cas systems, Nat. Rev. Microbiol. 3 (2014) 3–8.
[4] J. Reeks, J.H. Naismith, M.F. White, CRISPR interference: a structural perspective, Biochem. J. 453 (2013) 155–166.
[5] K.S. Makarova, D.H. Haft, R. Barrangou, S.J. Brouns, E. Charpentier, P. Horvath, S. Moineau, F.J. Mojica, Y.I. Wolf, A.F. Yakunin, J. van der Oost, E.V. Koonin,

Evolution and classification of the CRISPR-Cas systems, Nat. Rev. Microbiol. 9 (2011) 467–477.
[6] K.A. Datsenko, K. Pougach, A. Tikhonov, B.L. Wanner, K. Severinov, E. Semenova, Molecular memory of prior infections activates the CRISPR/Cas adaptive bacterial immunity system, Nat. Commun. 3 (2012) 945.
[7] I. Yosef, M.G. Goren, U. Qimron, Proteins and DNA elements essential for the CRISPR adaptation process in *Escherichia coli*, Nucleic Acids Res. 40 (2012) 5569–5576.
[8] R. Sapranauskas, G. Gasiunas, C. Fremaux, R. Barrangou, P. Horvath, V. Siksnys, The *Streptococcus thermophilus* CRISPR/Cas system provides immunity in *Escherichia coli*, Nucleic Acids Res. 39 (2011) 9275–9282.
[9] N. Beloglazova, G. Brown, M.D. Zimmerman, M. Proudfoot, K.S. Makarova, M. Kudritska, S. Kochinyan, S. Wang, M. Chruszcz, W. Minor, E.V. Koonin, A.M. Edwards, A. Savchenko, A.F. Yakunin, A novel family of sequence-specific endoribonucleases associated with the clustered regularly interspaced short palindromic repeats, J. Biol. Chem. 283 (2008) 20361–20371.
[10] P. Samai, P. Smith, S. Shuman, Structure of a CRISPR-associated protein Cas2 from *Desulfovibrio vulgaris*, Acta Crystallogr. Sect. F Struct. Biol. Cryst. Commun. 66 (2010) 1552–1556.
[11] K.H. Nam, F. Ding, C. Haitjema, Q. Huang, M.P. DeLisa, A. Ke, Double-stranded endonuclease activity in *Bacillus halodurans* clustered regularly interspaced short palindromic repeats (CRISPR)-associated Cas2 protein, J. Biol. Chem. 287 (2012) 35943–35952.
[12] Z. Otwinowski, W. Minor, Processing of X-ray diffraction data collected in oscillation mode, Method Enzymol. 276 (1997) 307–326.
[13] A.J. McCoy, R.W. Grosse-Kunstleve, P.D. Adams, M.D. Winn, L.C. Storoni, R.J. Read, Phaser crystallographic software, J. Appl. Crystallogr. 40 (2007) 658–674.
[14] P. Emsley, K. Cowtan, Coot: model-building tools for molecular graphics, Acta Crystallogr. D Biol. Crystallogr. 60 (2004) 2126–2132.
[15] G.N. Murshudov, A.A. Vagin, E.J. Dodson, Refinement of macromolecular structures by the maximum-likelihood method, Acta Crystallogr. D Biol. Crystallogr. 53 (1997) 240–255.
[16] V.B. Chen, W.B. Arendall 3rd, J.J. Headd, D.A. Keedy, R.M. Immormino, G.J. Kapral, L.W. Murray, J.S. Richardson, D.C. Richardson, MolProbity: all-atom structure validation for macromolecular crystallography, Acta Crystallogr. D Biol. Crystallogr. 66 (2010) 12–21.
[17] H.M. Berman, J. Westbrook, Z. Feng, G. Gilliland, T.N. Bhat, H. Weissig, I.N. Shindyalov, P.E. Bourne, The protein data bank, Nucleic Acids Res. 28 (2000) 235–242.
[18] M. Babu, N. Beloglazova, R. Flick, C. Graham, T. Skarina, B. Nocek, A. Gagarinova, O. Pogoutse, G. Brown, A. Binkowski, S. Phanse, A. Joachimiak, E.V. Koonin, A. Savchenko, A. Emili, J. Greenblatt, A.M. Edwards, A.F. Yakunin, A dual function of the CRISPR-Cas system in bacterial antivirus immunity and DNA repair, Mol. Microbiol. 79 (2011) 484–502.
[19] B. Wiedenheft, K. Zhou, M. Jinek, S.M. Coyle, W. Ma, J.A. Doudna, Structural basis for DNase activity of a conserved protein implicated in CRISPR-mediated genome defense, Structure 17 (2009) 904–912.
[20] J.K. Nunez, P.J. Kranzusch, J. Noeske, A.V. Wright, C.W. Davies, J.A. Doudna, Cas1–Cas2 complex formation mediates spacer acquisition during CRISPR-Cas adaptive immunity, Nat. Struct. Mol. Biol. 21 (2014) 528–534.